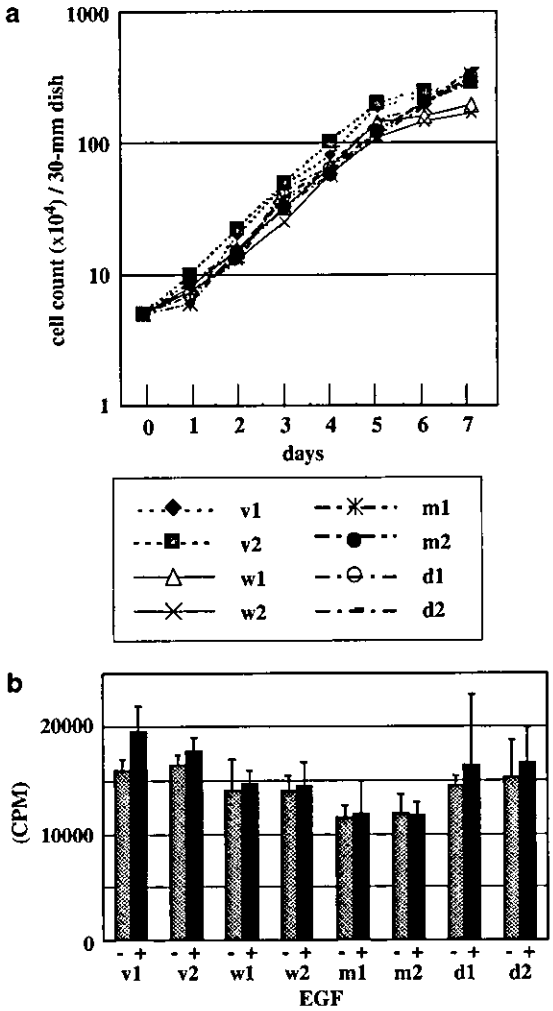

Figure 2 Growth rate and proliferation ability of ShcC mutant cells *in vitro*. (**a**) ShcC mutant cells cultured in a normal medium with 10% FCS by 30-mm dishes were counted at the indicated time points. The results represent the average values (±s.d.) of three replicated experiments for each clone. (**b**) ShcC mutant cells stimulated with none (gray bar) or EGF (black bar) were treated with [^{3}H]thymidine to the culture medium as described in Materials and methods. The graph represents the average values (±s.d.) from an experiment performed in triplicate. NB-39-nu clones are described as: v1 and v2 (control), w1 and w2 (expressing ShcC-wt), m1 and m2 (expressing 3YF), d1 and d2 (expressing ΔSH2)

that the anchorage-independent phosphorylation of Cas is associated with the activity of the SFKs (Figure 6f).

The activation of ERK1/2 or Akt was similarly suppressed by suspension culture for 24 h regardless of the expression of each ShcC mutants although the basal level is lower in 3YF-ShcC clones (Supplementary Figure A). There were no difference in phosphorylation level of FAK and paxillin, which plays an important role in regulating the signals from the extracellular matrix (ECM) and organizing the actin-cytoskeleton, by expressing ShcC-wt, showing a similar level of decrease in the suspended condition (Supplementary Figure B). In summary, it was confirmed in this system that the constitutive activation of SFKs, such as Fyn and c-Src, and phosphorylation of Cas in suspended cells, but not other components of integrin signals such as FAK, is strictly linked to the anchorage independency of NB-39-nu cells, closely related with ShcC mutants expression. Furthermore, we detected interaction between ShcC-wt and some of SFKs following the stimulation (Figure 6g), indicating a novel biological interaction of ShcC with SFK, as suggested for ShcA in integrin pathway (Wary *et al*., 1996; Giancotti, 1997)

Loss of tumorigenicity of NB-39-nu-expressing ShcC-wt or 3YF-ShcC in mouse subcutaneous tissues

To investigate these antitransforming effects of ShcC-wt and 3YF-ShcC *in vivo*, the tumorigenicity of NB-39-nu cells expressing each mutant in nude mice was evaluated. Tumors generated by eight independent injections of each mutant were analysed in weight and histology at 4 weeks after subcutaneous injection. The results revealed a marked reduction in sizes of tumors from the cells expressing either ShcC-wt or 3YF-ShcC at this time, but not of tumors from the control cells or cells expressing ΔSH2-ShcC (Figure 7a).

The tumors from the control, ShcC-wt-expressing and ΔSH2-ShcC-expressing cells presented a hypervascular appearance (Figure 7a: upper panel), which has the histological characteristics of almost equal-sized cells with a regular arrayed pattern, high nuclear-to-cytoplasmic (N/C) ratio and chromatin-rich nucleuses (Figure 7b). On the other hand, the tumors from the 3YF-ShcC-expressing cells were hypovascular and histologically distinct from the other mutants, showing rather unequal-sized cells with an irregular arrayed pattern, a lower N/C ratio, few mitosis and decreased nucleus density. In accordance with this, staining by a proliferation marker, Ki-67, or a mitotic activity marker, cyclin A, markedly decreased in the tumors from 3YF-ShcC-expressing cells (Figure 7b), showing that the cell cycle progression was significantly suppressed by 3YF-ShcC *in vivo*, compared with the analysis by [^{3}H]-tymidine incorporation *in vitro* (Figure 2b). TUNEL staining showed no marked difference in cell apoptosis among each tumor tissue (data not shown). These results suggest that the antitumorigenic activity of the 3YF-ShcC-expressing cells *in vivo* accompanies the regulation of cell proliferation, which is distinct from the impairment of tumorigenicity by expression of ShcC-wt.

Discussion

In our previous report, the biological effects of constitutively activated signals of ALK-ShcC on the tumorigenesis of neuroblastoma cells remain to be investigated. Here, we demonstrated that the proliferation, survival and cell migration of these neuroblastoma cells were dependent on the signals via ShcC-Grb2 pathway, downstream of ALK. Additionally, overexpressed ShcC has a suppressive effect on the

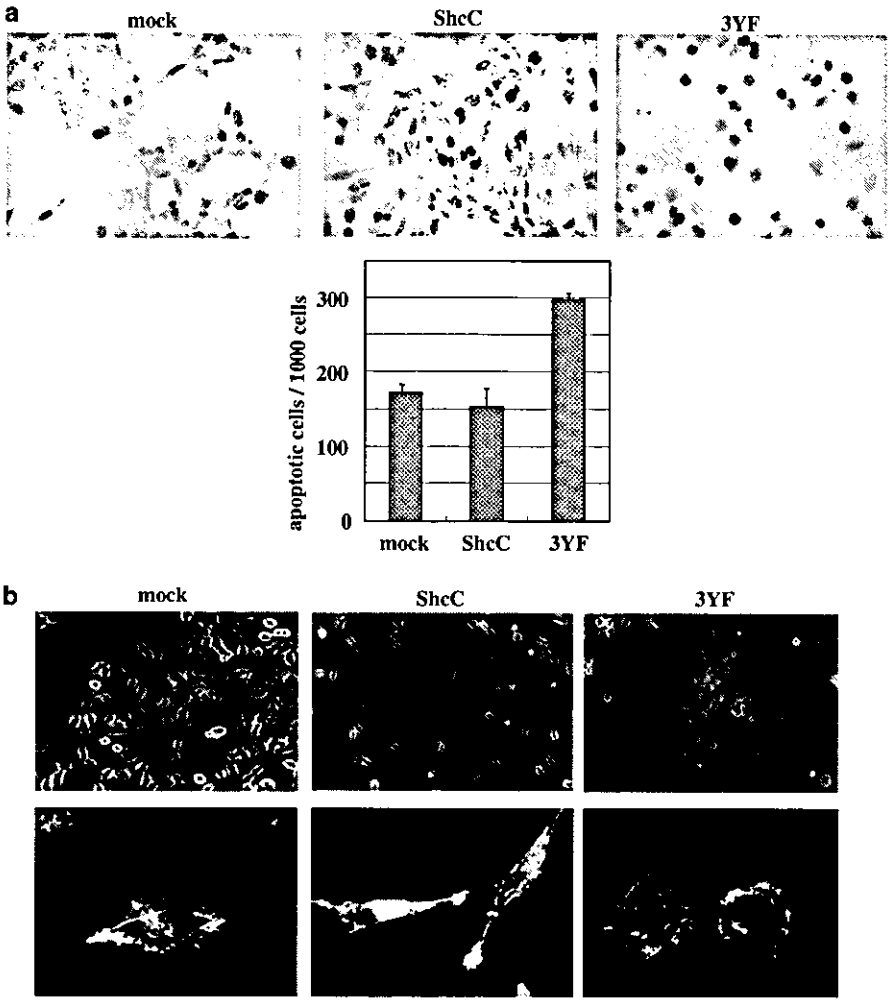

Figure 3 Effects of ShcC mutants on apoptosis and differentiation of NB-39-nu cells induced by all-*trans* retinoic acid (RA). (**a**) TUNEL analysis of ShcC mutant cells were performed as described in Materials and methods. Bar: 100 μm (upper panel). TUNEL-positive cells, the prominent dark positive cells, are counted for every 1000 cells for each slide, and three different slides were analysed for each sample. The graph represents the results (expressed as mean $\pm$ s.d.) of three observations (lower panel). (**b**) RA-induced morphological change of NB-39-nu cells expressing ShcC mutants. The cells were grown for 48 h in RPMI 1640 with 10% FCS containing 2.5 μM of RA and examined by phase-contrast microscopy (upper panel). Actin filaments stained with FITC-labeled phalloidin were visualized with a confocal fluorescence microscope (lower panel)

anchorage-independent growth of these cells via its SH2 domain and this regulation is closely associated with the regulation of c-Src and Fyn tyrosine kinases.

The fact that 3YF-ShcC significantly suppressed the activity of both ERK1/2 and Akt, suggesting that ShcC, among signaling pathways originating from activated ALK, predominantly regulates these signals through binding to Grb2. Our recent study also shows that the suppression of activated ALK using the RNA interference technique (RNAi) reduces the phosphorylation of ShcC, ERK1/2 and Akt, and induces the apoptotic cell death of NB-39-nu cells (Hakomori *et al.*, manuscript in preparation). The ERK and Akt pathways are key regulators of cell proliferation, survival and differentiation. Cells expressing 3YF-ShcC become more susceptible to RA-induced apoptosis presumably due to inhibition of the Akt pathway. It has recently been shown that ShcC is physiologically involved in the regulation of the PI3K/Akt pathway as a downstream effecter of the ligand-stimulated Ret receptor in neuroblastoma cells (Pelicci *et al.*, 2002). This study confirms that the survival of NB-39-nu cells is regulated by the signals downstream of ShcC. The 3YF-ShcC also causes inhibition of cell motility, while overexpressed ShcC significantly increases the ability of cell migration, indicating that ShcC positively affects the regulation of cell migration. Previously, ShcA was shown to be closely related with cell motility via the MAPK pathway (Collins *et al.*, 1999; Gu *et al.*, 1999), but the association of ShcC with the ability of cell migration has not been investigated.

The expression of 3YF-ShcC had a suppressive effect on the proliferation of NB-39-nu cells cultured *in vitro* and more significantly on the cell cycle progression of

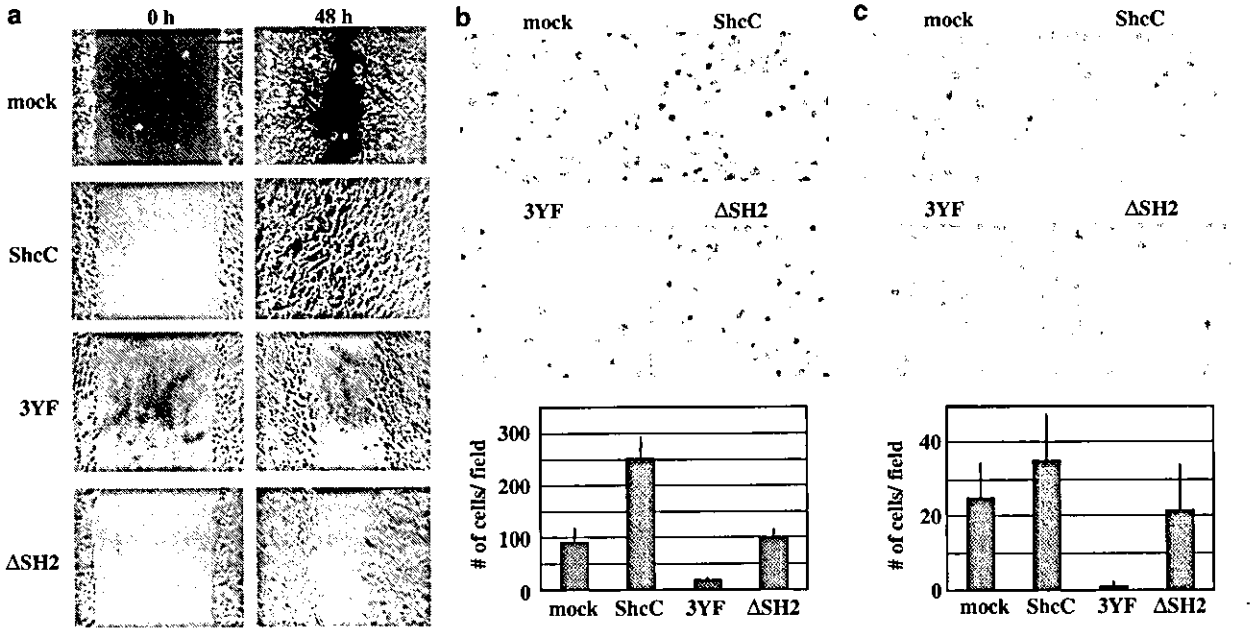

Figure 4 Expression of ShcC-wt significantly promotes the ability of cell migration in NB-39-nu cells. (**a**) Wound-healing assay for ShcC mutant cells. Photographs of the cells taken 48 h after wounding under a microscope. Bar: 200 μm. (**b**) Photographs (upper panel) and graph (lower panel) of ShcC mutant cells that have migrated through the filter by modified Boyden chamber cell migration assay. The graph represents the results (expressed as mean $\pm$ s.d.) of the experiments performed in triplicate. (**c**) Photographs (upper panel) and a graph (lower panel) of the results from cell invasion assay

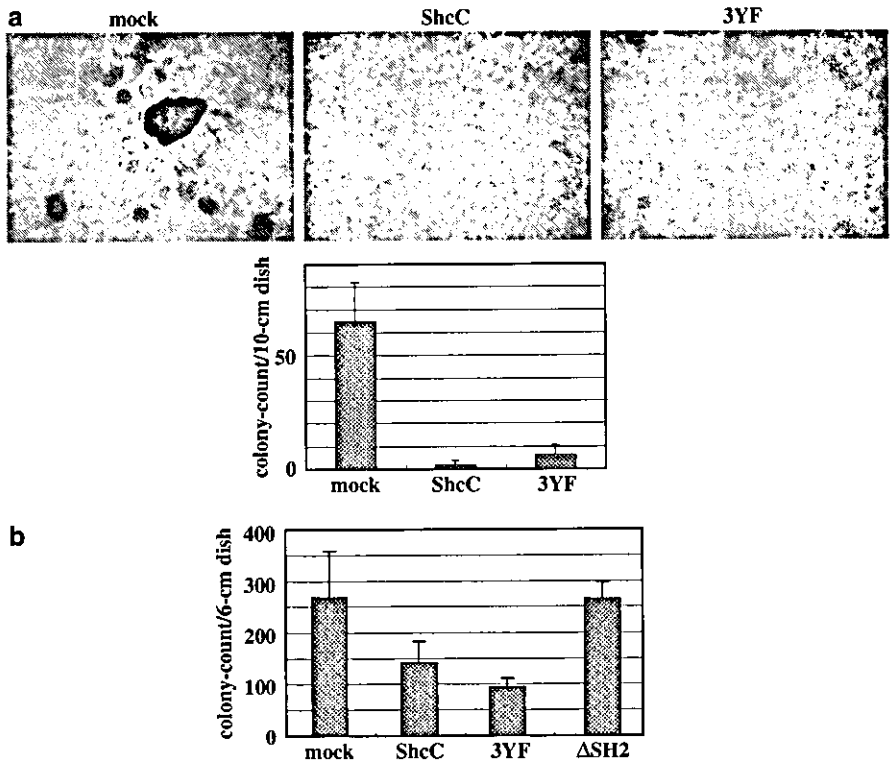

Figure 5 Evaluation of *in vitro* transforming activity in NB-39-nu cells expressing ShcC mutants. (**a**) Tendency for ShcC mutant cells to form cell aggregations on the dish surface as described in Materials and methods. Photographs of each dish were taken with a microscope at a magnification of $\times$ 40 (upper panel). The graph represents the mean values ($\pm$ s.d.) of three independent experiments (lower panel). (**b**) Anchorage-independent growth of ShcC mutant cells was evaluated by assaying colony formation in soft agar (performed as described in Materials and methods). The results represent the average values ($\pm$ s.d.) of three replicated experiments

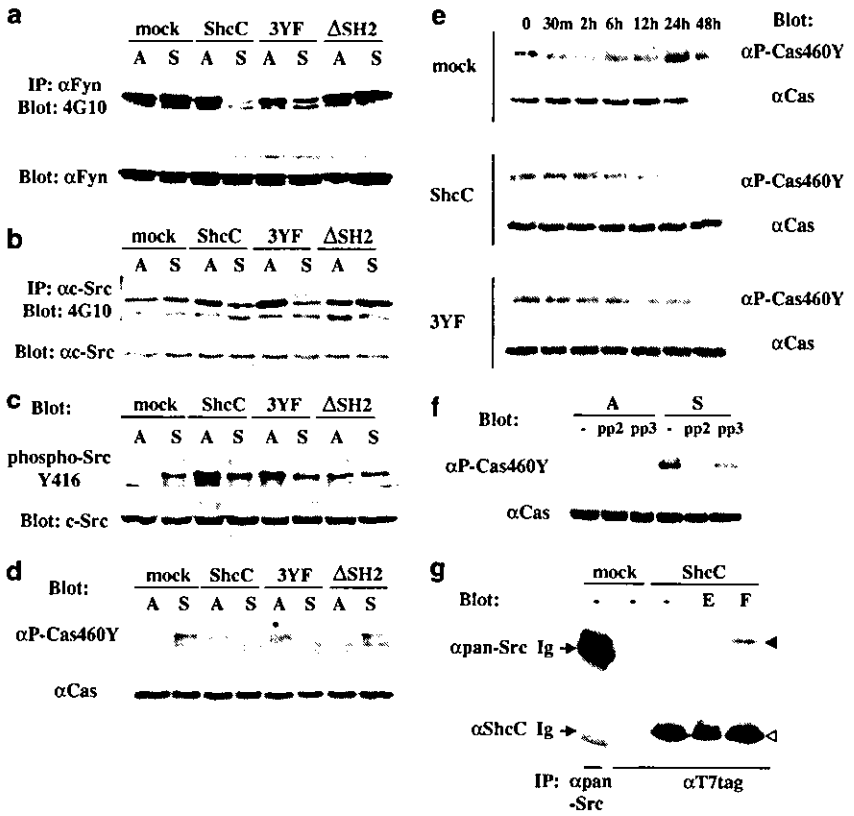

Figure 6 Anchorage-independent activation of Src family kinases (SFKs) and tyrosine phosphorylation of Cas in NB-39-nu is affected by the expression of ShcC. The cell suspension culture of ShcC mutant cells was essentially performed as described in Materials and methods. A: attached cells. S: cells in a suspended condition. Lysates were duplicated and detected by immunoprecipitation and Western analysis. (**a**, **b** and **c**) Cells cultured for 24 h in adherent or suspended conditions were analysed with the antibodies against each Src family kinase shown in the figure. Anti-phospho-Src Y416 recognizes all Src family members phosphorylated at the tyrosine corresponding to Tyr416 of avian Src. (**d**) Same analysis performed as (**a**) (**b**) and (**c**) using the antibodies against for phospho-460Y of Cas (αP-Cas460Y) and Cas protein (αCas). (**e**) Time course of tyrosine phosphorylation of Cas in each ShcC mutant cells cultured in suspension for the indicated time periods. (**f**) Effect of Src inhibitor, PP2, on the tyrosine phosphorylation of Cas in NB-39-nu control cells. The cells cultured for 24 h were harvested following treatment with 10 μM of PP2 for 2 h. As a negative control, the same dose of PP3 was used in place of PP2. (**g**) ShcC forms complex with SFKs following the stimulation of fibronectin. Lysates of mock cells and ShcC-wt cells were analysed after the stimulation with EGF or fibronectin as described in Materials and methods. -: serum free without stimulation; E: stimulated by EGF; F: stimulated by fibronectin. Ig: immunoglobulin. Anti-pan-Src antibody (SRC2) reacts with c-Src p60, Yes p62, Fyn p59, c-Fgr p55 and c-Src2. closed arrowhead: SFK; open arrowhead: p52 ShcC

the nude mouse tumor. These data suggest that ShcC positively regulates the cell proliferation of neuronal tumor cells as well as ShcA, which has been reported to affect the tumor growth in nude mice using breast cancer cell lines (Stevenson *et al.*, 1999).

The overexpression of ShcC-wt endowed NB-39-nu cells with several characteristics. Other than the enhancement of cell migration and neurite outgrowth, which is consistent with previous study (Collins *et al.*, 1999; Pelicci *et al.*, 2002), the observation that ShcC-wt-expressing cells were impaired for anchorage-independent growth and tumorigenicity suggests a novel function of ShcC. Taking into account that the expression of 3YF-ShcC but not ΔSH2-ShcC showed similar effects, the SH2 domain of ShcC may be responsible for this unique function of ShcC, distinct from ShcA. In addition, the least changes in ERK1/2 or Akt activation by overexpression of ShcC-wt suggest that this function might be independent of phosphorylation of Grb2-binding sites or the activation levels of downstream targets. There are reports showing different binding specificity towards phosphotyrosine-containing motifs among Shc families (O'Bryan *et al.*, 1996a, b; Pelicci *et al.*, 1996). It is crucial to identify the molecules associating with the SH2 domain of ShcC in neuroblastoma cells to elucidate the mechanism of these SH2-mediated effects of ShcC.

The smaller size of the nude mouse tumors due to the expression of ShcC-wt, regardless of mild changes in cell proliferation as both tumor tissue and culture cells, may also reflect suppression of anchorage independency (Freedman and Shin, 1974; Kumar, 1998), which results in the loss of the majority of the injected cells by anoikis before they start forming tumors. The anchorage independency of NB-39-nu mutants well corresponded to the sustained phosphorylation levels of c-Src, Fyn

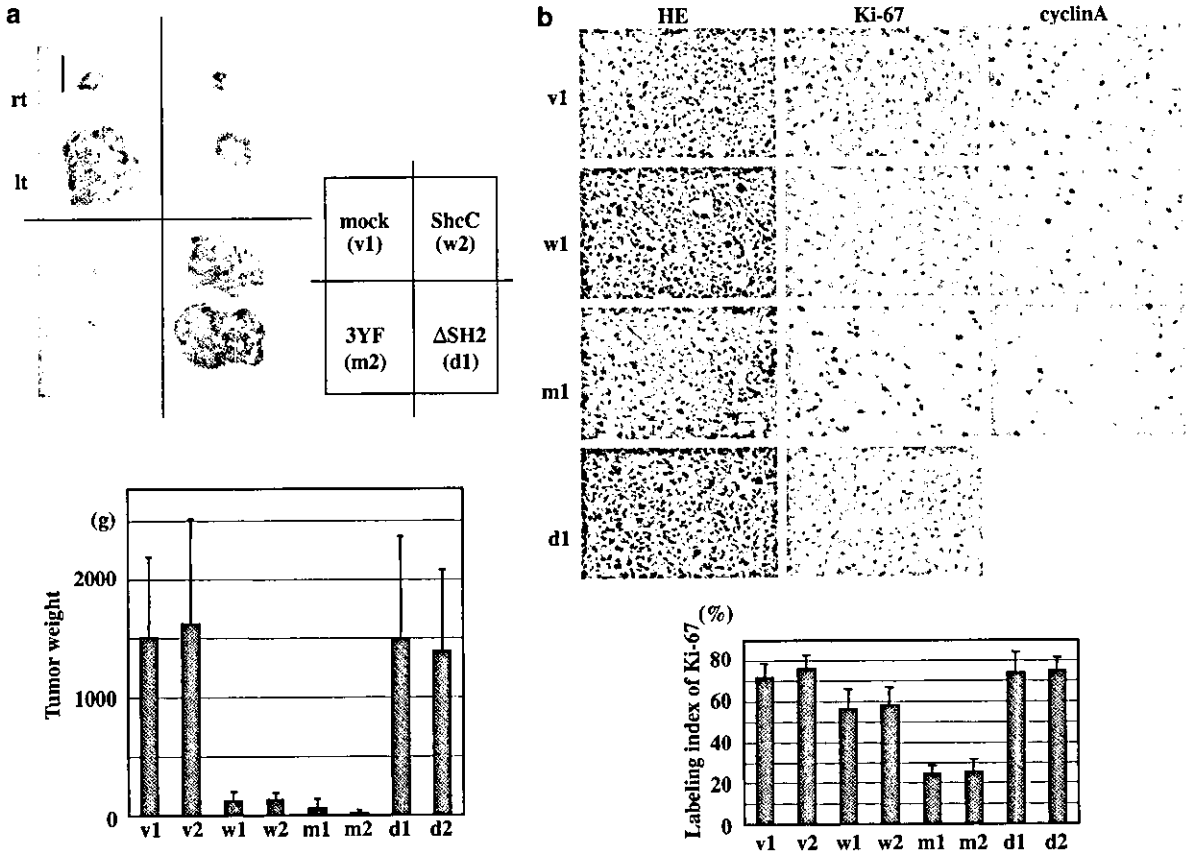

Figure 7 Nude mouse tumors derived from ShcC mutant cells. (**a**) Photographs of tumors from nude mice at three weeks after subcutaneous injection of ShcC mutant cells (upper panel). Tumorigenicity shown by the average weight (±s.d.) of the eight tumors derived from each clone (lower panel). Two independent clones are analysed for each ShcC mutant. Bar: 10 mm (**b**) Photographs of a cross-section of each tumor tissue using a microscope at a magnification of ×400. HE: tumor tissues stained with hematoxylin and eosin; Ki-67 and cyclin-A: tumor tissues immunostained against Ki-67 and cyclin-A, respectively (upper panels). The proliferating activity of each tumor was defined as the labeling index of Ki-67 by counting the positive stained cells per 1000 tumor cells. The data show the average scores ± s.d. of the positive cells in three different areas of each slide (lower panel). NB-39-nu clones are described as: v1 and v2 (control), w1 and w2 (expressing ShcC-wt), m1 and m2 (expressing 3YF-ShcC), d1 and d2 (expressing ΔSH2-ShcC)

and Cas after cell detachment, suggesting that the expression of ShcC-wt has a negative effect on anchorage independency due to the suppression of the SFK-Cas pathway (Figure 6). It is possible that ShcC-SH2 plays a competitive role with YDYV in the Src-binding domain of Cas, judging from the consensus motifs binding to ShcC-SH2 (O'Bryan *et al*., 1996a, b), although this association was not detected by usual immunoprecipitation experiments (data not shown). On the other hand, the fact that ShcC forms the complex with SFK in this study indicates that there might be a role of association between SFK and ShcC in the regulation of tyrosine kinase activity of SFK. The fact that malignant neuroblastoma cell lines with hyperphosphorylated ShcC frequently have lower expression level of ShcC (Miyake *et al*., 2002) might indicate additive effects of hyperphosphorylation and downregulation of ShcC on phenotype of neuroblastoma. There is the possibility that an unknown mechanism causes down-regulation of ShcC, which is hyperphosphorylated by receptor stimulation, and eventually induces malignant transition of tumors.

We have shown in this study that hyperphosphorylated ShcC in neuroblastoma cells plays an essential role in regulating cellular proliferation, survival, migration and transformation, and each domain of ShcC might differentially regulate these physiological functions. Controlling these domain-mediated signals could be a target in restricting the progression and metastasis of neuroblastoma cells.

Materials and methods

Plasmid constructions

The full-length human ShcC cDNA for transfection was donated by Dr T Nakamura (Nakamura *et al*., 1996b), and inserted into a mammalian expression vector pcDNA3.1. Tyrosine-to-phenylalanine mutations were introduced in the ShcC cDNAs by *in vitro* site-directed mutagenesis, which changed Y221/222 and Y304 to three phenylalanines (3YF-ShcC). The SH2 domain (amino acid 379–472)-deleted form of

ShcC (ΔSH2-ShcC) was also generated. All parts amplified by PCR were verified by sequencing.

Cell culture, transfection

NB-39-nu cells were used in our previous report (Miyake *et al.*, 2002). The stable expression of ShcC mutants, the full-length of ShcC (ShcC-wt), 3YF-ShcC and ΔSH2-ShcC in NB-39-nu cells were obtained by transfection using Fugene™ 6 transfection reagent (Roche Molecular Biochemicals) according to the manufacturer's instructions. Then, cell clones were obtained from individual G418-resistent colonies and subjected to Western blot screening using the T7 tag antibody (Novagen). These cells were cultured in an RPMI 1640 medium with 10% FCS (Sigma) at 37°C in 5% CO_2. A suspension culture of the cells was essentially performed according to a previously published procedure (Folkman and Moscona, 1978; Frisch and Francis, 1994; Wang and Sheibani, 2002). In this study, LOW-CELL-BINDING 90 mm-Petri dishes treated with 2-Methacryloxyethyl Phosphorylcholine (MPC) (Nalge Nunc International) were used instead of poly-HEMA-coated dishes. The cells were grown to confluence in tissue culture dishes, and were then trypsinized and plated at a concentration of 1×10^6 cells/90 mm dish into MPC-treated Petri dishes and cultured for 0–48 h. The cells were then collected by pipetting, washed by PBS and extracted with PLC-lysis buffer (Rozakis-Adcock *et al.*, 1993) for the Western analysis.

Preparation of specific antibodies, cell stimulation, immunoprecipitation and immunoblotting

The polyclonal antibodies against the CH1 domains of ShcC (amino acid 306–371) and against Cas protein (αCas) were prepared as described (Sakai *et al.*, 1994, 2000). A phospho specific polyclonal antibody against Cas (αP-Cas460Y) was generated by immunizing rabbits with a synthetic peptide, CAEDV(pY)DVP, which is a representative of the repetitive tyrosine-containing motifs in the substrate domain of Cas, after being conjugated with thyroglobulin. Other antibodies were purchased as follows: anti-phosphotyrosine antibody (4G10) (Upstate Biotechnology, Inc), anti-p44/42 MAPK (ERK1/2) and anti-phospho-p44/42 MAPK (phospho-ERK1/2) antibodies (BioLabs), anti-Akt and anti-phospho-Akt (Ser473) antibodies (Cell Signaling), anti-c-Src antibody (Upstate Biotechnology, Inc.), anti-phospho Src family (Tyr416) antibody (Cell Signaling), anti-Fyn antibody and anti-pan-Src antibody (SRC2) (SantaCruz Biotechnology, Inc.). As secondary antibodies, horseradish peroxidase (HRP)-conjugated anti-rabbit and anti-mouse Ig (Amersham) were used. Cell-stimulation analysis with epidermal growth factor (EGF; Wako) was performed as described. The cells were starved for 24 h and treated for 5 min with EGF (100 ng/ml) (Miyake *et al.*, 2002). As for stimulation with fibronectin, cultured cells were starved for 24 h then trypsinized without FCS and after the suspending condition for 30 min, seeded onto fibronectin (10 μg/ml)-coated dishes and harvested after 1 h using PLC lysis buffer. Control cells were harvested before the attachment on the fibronectin-coated surface. The immunoprecipitation and Western analysis were performed using the procedure described in the previous report (Miyake *et al.*, 2002).

Evaluation of tendency to form cell aggregations on dish surface

Cells were seeded onto plastic dishes (1×10^6 cells per 100-mm diameter dish). After 5 days, distinctive colonies of cell aggregations proliferated independently of the attachment to the dish surface, and each of them consisted of more than 10 cells per dish. The data were obtained from three independent experiments.

Soft agar colony-formation assay

Anchorage-independent growth was determined by assaying colony formation in soft agar as described in the previous report (Honda *et al.*, 1998). Briefly, 10^5 trypsinized cells were resuspended in DMEM containing 10% FCS and 0.4% Sea Plaque GTG agarose (Bioproduct) and poured onto bottom agar containing 10% FCS and 0.53% agarose in 6-cm culture dishes. The cells were then incubated at 37°C with 5% CO_2. After 14 days, colonies containing more than five cells were counted under the microscope.

Wound-healing assay

A wound-healing assay was performed according to the method used previously (Honda *et al.*, 1999). Briefly, cells were grown to confluence in Matrigel-coated plastic culture dishes, and a wound was made using a sterile micropipette tip. Cell movement was assessed 24 and 48 h after wounding under the microscope at a magnification of × 100.

Cell migration and invasion assay

Cell invasion was analysed according to the procedure of the Boyden chamber cell migration assay with some modification (Honda *et al.*, 1999), using a FALCON™ Cell Culture Insert, a chamber with a pore size of 8 μm (Becton Dickinson Labware) whose interior was filled with a plug of 10 μg Matrigel (IWAKI) per filter. A total of 1×10^5 cells in 200 μl of serum-free medium were plated in the Matrigel chamber, and a serum-free medium containing 50 μg/ml of fibronectin was placed in the 24-well plate as a lower chamber, then incubated for 12 h at 37°C in 5% CO_2. The number of cells migrated through the Matrigel to the underside of the filter was counted under the microscope. The same procedure was performed without Matrigel coating for the analysis of cell migration.

*Apoptosis of neuroblastoma cells induced by all-*trans *RA*

Cells, were seeded into 24-well tissue culture plates at a density of $5 \times 10^4\,cm^{-2}$ and cultured in the presence of the indicated concentration of RA (all-*trans* form; Sigma) dissolved in 70% ethanol. Control cultures were treated with the same concentration of ethanol. To identify RA-induced apoptotic reaction, TUNEL (TdT-mediated dUTP-biotin nick end labeling) was performed according to the manufacturer's instructions (In Situ Cell Death Detection, POD: Roche) as described by Gavrieli *et al.* (1992). The cells were counterstained with hematoxylin-eosin.

[^{3}H]thymidyne incorporation assay

This was performed essentially as described previously (McNeil *et al.*, 1985). A total of 2×10^4 cells were seeded onto 24-well dishes and cultured for 48 h and shifted to a serum-free medium, and then 24 h later were followed by overnight stimulation with 100 ng/ml EGF. [^{3}H]thymidine (1 μCi/ml) was added for the last 4 h of incubation. The amount of incorporated [^{3}H]thymidine radioactivity was measured by liquid scintillation counting. Results are expressed as disintegrations per minute of incorporated [^{3}H]thymidine per well.

Generation of tissue samples and histological evaluation

Nude mouse tumors were obtained by independent injections of 5×10^6 ShcC mutant cells into the bilateral subcutaneous tissues of each mouse. Tumor tissues were fixed in formalin at 4°C, transferred to 70% ethanol, and blocked in paraffin. Sections were stained with hematoxylin and eosin.

Immunohistochemistry

The sections of the tumor tissues from ShcC mutant cells were immunostained with anti-Ki-67 antibody (DAKO) and anti-cyclin-A antibody (Novocastra Laboratories) using the labeled streptavidin biotin (LSAB) methods according to the manufacturer's instructions of the LSAB kit (Dako). All the primary antigens were used at a 1 : 100 dilution. Peroxidase activity was visualized with 3, 3′-diaminobebenzidine (DAB).

Acknowledgements
This study was supported by the Program for Promotion of Fundamental Studies in Health Sciences of Organization for Pharmaceutical Safety and Research of Japan, and was also supported by a grant from SBS, Inc. Izumi Miyake is the recipient of Research Resident Fellowships from the Japan Health Sciences Foundation.

References

Andrechek ER, Hardy WR, Siegel PM, Rudnicki MA, Cardiff RD and Muller WJ. (2000). *Proc. Natl. Acad. Sci. USA*, **97**, 3444–3449.
Collins LR, Ricketts WA, Yeh L and Cheresh D. (1999). *J. Cell Biol.*, **147**, 1561–1568.
Folkman J and Moscona A. (1978). *Nature*, **273**, 345–349.
Freedman VH and Shin SI. (1974). *Cell*, **3**, 355–359.
Frisch SM and Francis H. (1994). *J. Cell Biol.*, **124**, 619–626.
Gavrieli Y, Sherman Y and Ben-Sasson SA. (1992). *J. Cell Biol.*, **119**, 493–501.
Giancotti FG. (1997). *Curr. Opin. Cell. Biol.*, **9**, 691–700.
Gu J, Tamura M, Pankov R, Danen EH, Takino T, Matsumoto K and Yamada KM. (1999). *J. Cell Biol.*, **146**, 389–403.
Honda H, Nakamoto T, Sakai R and Hirai H. (1999). *Biochem. Biophys. Res. Commun.*, **262**, 25–30.
Honda H, Oda H, Nakamoto T, Honda Z, Sakai R, Suzuki T, Saito T, Nakamura K, Nakao K, Ishikawa T, Katsuki M, Yazaki Y and Hirai H. (1998). *Nat. Genet.*, **19**, 361–365.
Iwahara T, Fujimoto J, Wen D, Cupples R, Bucay N, Arakawa T, Mori S, Ratzkin B and Yamamoto T. (1997). *Oncogene*, **14**, 439–449.
Kumar CC. (1998). *Oncogene*, **17**, 1365–1373.
McNeil PL, McKenna MP and Taylor DL. (1985). *J. Cell Biol.*, **101**, 372–379.
Miyake I, Hakomori Y, Shinohara A, Gamou T, Saito M, Iwamatsu A and Sakai R. (2002). *Oncogene*, **21**, 5823–5834.
Morris SW, Naeve C, Mathew P, James PL, Kirstein MN, Cui X and Witte DP. (1997). *Oncogene*, **14**, 2175–2188.
Nakamura N, Chin H, Miyasaka N and Miura O. (1996a). *J. Biol. Chem.*, **271**, 19483–19488.
Nakamura T, Sanokawa R, Sasaki Y, Ayusawa D, Oishi M and Mori N. (1996b). *Oncogene*, **13**, 1111–1121.
O'Bryan JP, Martin CB, Songyang Z, Cantley LC and Der CJ. (1996a). *J. Biol. Chem.*, **271**, 11787–11791.
O'Bryan JP, Songyang Z, Cantley L, Der CJ and Pawson T. (1996b). *Proc. Natl. Acad. Sci. USA*, **93**, 2729–2734.
Parsons JT and Weber MJ. (1989). *Curr. Top. Microbiol. Immunol.*, **147**, 79–127.
Pawson T, Gish GD and Nash P. (2001). *Trends Cell Biol.*, **11**, 504–511.
Pelicci G, Dente L, De Giuseppe A, Verducci-Galletti B, Giuli S, Mele S, Vetriani C, Giorgio M, Pandolfi PP, Cesareni G and Pelicci PG. (1996). *Oncogene*, **13**, 633–641.
Pelicci G, Lanfrancone L, Grignani F, McGlade J, Cavallo F, Forni G, Nicoletti I, Pawson T and Pelicci PG. (1992). *Cell*, **70**, 93–104.
Pelicci G, Troglio F, Bodini A, Melillo RM, Pettirossi V, Coda L, De Giuseppe A, Santoro M and Pelicci PG. (2002). *Mol. Cell. Biol.*, **22**, 7351–7363.
Rozakis-Adcock M, Fernley R, Wade J, Pawson T and Bowtell D. (1993). *Nature*, **363**, 83–85.
Sakai R, Henderson JT, O'Bryan JP, Elia AJ, Saxton TM and Pawson T. (2000). *Neuron*, **28**, 819–833.
Sakai R, Iwamatsu A, Hirano N, Ogawa S, Tanaka T, Mano H, Yazaki Y and Hirai H. (1994). *EMBO J.*, **13**, 3748–3756.
Sidell N, Altman A, Haussler MR and Seeger RC. (1983). *Exp. Cell Res.*, **148**, 21–30.
Stevenson LE, Ravichandran KS and Frackelton Jr AR. (1999). *Cell Growth Differ.*, **10**, 61–71.
Thomas D and Bradshaw RA. (1997). *J. Biol. Chem.*, **272**, 22293–22299.
van der Geer P, Wiley S, Gish GD and Pawson T. (1996). *Curr. Biol.*, **6**, 1435–1444.
van der Geer P, Wiley S, Lai VK, Olivier JP, Gish GD, Stephens R, Kaplan D, Shoelson S and Pawson T. (1995). *Curr. Biol.*, **5**, 404–412.
Wang Y and Sheibani N. (2002). *J. Cell. Biochem.*, **87**, 424–438.
Wary KK, Mainiero F, Isakoff SJ, Marcantonio EE and Giancotti FG. (1996). *Cell*, **87**, 733–743.
Wary KK, Mariotti A, Zurzolo C and Giancotti FG. (1998). *Cell*, **94**, 625–634.
Wei L, Yang Y, Zhang X and Yu Q. (2002). *J. Cell. Biochem.*, **87**, 439–449.
Weng Z, Thomas SM, Rickles RJ, Taylor JA, Brauer AW, Seidel-Dugan C, Michael WM, Dreyfuss G and Brugge JS. (1994). *Mol. Cell. Biol.*, **14**, 4509–4521.
Windham TC, Parikh NU, Siwak DR, Summy JM, McConkey DJ, Kraker AJ and Gallick GE. (2002). *Oncogene*, **21**, 7797–7807.

Supplementary Information accompanies the paper on Oncogene website (http://www.nature.com/onc).

Oncogene (in press)

Tyrosine phosphorylation of paxillin affects the metastatic potential of human osteosarcoma

Kotaro Azuma[1,2], Masamitsu Tanaka[1], Takamasa Uekita[1], Satoshi Inoue[2], Jun Yokota[3], Yasuyoshi Ouchi[2], Ryuichi Sakai[1]*

[1]Growth Factor Division and [3]Division of Biology, National Cancer Center Research Institute, 5-1-1 Tsukiji, Chuo-ku, Tokyo 104-0045, Japan; [2]Department of Geriatric Medicine, Graduate School of Medicine, The University of Tokyo, 7-3-1, Hongo, Bunkyo-ku, 113-8655, Tokyo, Japan.

Running Title: Paxillin phosphorylation in human osteosarcoma

Keywords: osteosarcoma, pulmonary metastasis, paxillin, tyrosine phosphorylation, Src family kinase, motility

*Address correspondence to: Growth Factor Division, National Cancer Center Research Institute, 5-1-1 Tsukiji, Chuo-ku, Tokyo 104-0045, Japan. Tel: (81)-3-3542-2511 (ext. 4300); Fax: (81)-3-3542-8170; E-mail: rsakai@gan2.res.ncc.go.jp.

The abbreviations used are:
BSA, bovine serum albumin; Cas, Crk-associated substrate; FAK, focal adhesion kinase;
FBS, fetal bovine serum; PBS, phosphate-buffered saline;
PP2, 4-amino-5-(4-chlorophenyl)-7-(t-butyl)pyrazolo[3,4-d]pyrimidine;
PP3, 4-amino-7-phenylpyrazol [3,4-d]pyrimidine; RNAi, RNA interference;
SH2, Src homology 2 domain; siRNA, short interfering RNA

Abstract

To acquire information on signal alteration corresponding to the changes in metastatic potential, we analyzed protein tyrosine phosphorylation of low- and high-metastatic human osteosarcoma HuO9 sublines, which were recently established as the first metastatic model of human osteosarcoma. Tyrosine phosphorylation of proteins around 60 kDa, 70 kDa, and 120-130 kDa was enhanced in high-metastatic sublines. Among these proteins, the protein around 70 kDa, which was most remarkably phosphorylated, was identified as paxillin, a scaffold protein in integrin signaling. Activity of Src family kinase correlated well with metastatic potential, and a Src family kinase inhibitor, PP2, not only abolished tyrosine phosphorylation of paxillin but also impaired the motility of high-metastatic sublines. The expression of paxillin was also elevated in high-metastatic sublines, and knocking down of paxillin expression by RNAi method resulted in attenuated motility of high-metastatic cells. We also demonstrated that the phosphorylated form of paxillin is essential for the migration promoting effect in human osteosarcoma. These findings suggest that enhanced activity of Src family kinases and overexpression of paxillin synergistically contribute to the high metastatic potential of human osteosarcoma through the hyperphosphorylation of paxillin.

Introduction

Multiple steps of tumor metastasis are regulated by various external stimuli such as hormones, cytokines and extracellular matrices. As major mediators of these stimuli, both receptor and non-receptor tyrosine kinases play important roles to elicit intracellular signal transduction in response to the metastatic environment of tumor cells (Pawson, 2004). Various processes such as cell adhesion, anchorage independent growth, cell motility, and cell invasion, which are essential components of tumor metastasis, are regulated by tyrosine phosphorylation. Indeed, the activation of Src family tyrosine kinases is frequently found during proliferation and metastasis of human cancers (Yeatman, 2004), indicating that tumor progression is reflected by the activity of tyrosine kinase and phosphorylation states of substrates in metastatic tumors.

Osteosarcoma is a primary malignant bone tumor that usually affects teenagers and frequent metastasis to the lungs is a clinical characteristic of osteosarcoma. As many as 20% of patients are estimated to have pulmonary metastases at the time of diagnosis and their prognosis is extremely poor with 10 to 20% 5-year survival rate (Meyers et al., 1993; Tsuchiya et al., 2002). Even though patients did not have metastases at the time of diagnosis, 35 to 50% of them developed pulmonary metastases during treatment (Huth & Eilber, 1989; Ward et al., 1994). For this reason, pulmonary metastasis of osteosarcoma requires effective prevention and treatment.

Investigation of pulmonary metastasis of human osteosarcoma was impeded by the lack of a proper metastatic model of human osteosarcoma cell lines. Recently Kimura et al. established human osteosarcoma cell lines with high metastatic potential to the lungs for the first time (Kimura et al., 2002). From parental HuO9 cells, M112 and M132 were established as high-metastatic sublines, which developed more than 200 macroscopic metastatic nodules in the lungs after injection of 2_10^6 cells into the tail vein of nude mice. On the other hand, L12 and L13 are low-metastatic sublines established by the dilution plating method from the same parent HuO9 cells (Nakano et al., 2003). These sublines developed only 0 to 15 macroscopic nodules in the lungs after injection of 2_10^6 cells and all mice survived up to 200 days.

In order to acquire information on signal alteration corresponding to the changes in metastatic potential, we compared the profile of protein tyrosine phosphorylation by utilizing these HuO9 derived sublines. A 68 kDa cytoskeletal protein, paxillin, was identified as a molecule that shows the most outstanding difference in phosphorylation state between low- and high-metastatic sublines among several phosphotyrosine-containing proteins that are differentially phosphorylated in these sublines. Paxillin has no intrinsic enzymatic activity, but it has multiple domains that interact with cytoskeletal and signaling molecules, and functions as a scaffold protein at focal adhesions (Schaller, 2001; Turner, 2000). Paxillin contains two critical tyrosine phosphorylation sites at Tyr 31 and Tyr 118 (Schaller & Parsons, 1995). These phosphotyrosines are considered to serve as docking sites for other signaling molecules, but it remains controversial whether these phosphotyrosines have promoting effect or inhibitory effect on cell motility.

In this study, we show overexpression and hyperphosphorylation of paxillin in high-metastatic sublines of human osteosarcoma, indicating that, in the case of human osteosarcoma, tyrosine phosphorylation of paxillin has a promoting effect for cell migration. We also demonstrate that elevated activity of Src family kinases in high-metastatic sublines is essential for the enhanced motility for these osteosarcoma cells, suggesting the contribution of Src family kinase activity to the high metastatic potential of human osteosarcoma.

Results

General enhancement of tyrosine phosphorylation in high-metastatic HuO9 sublines

First, we confirmed the difference in motility between low- and high-metastatic sublines using Cell Culture Insert. High-metastatic sublines, M112 and M132, showed more than six times as high motility as low-metastatic sublines, L12 and L13 (data not shown). This result indicates that the motility of HuO9 sublines indeed correlates with their metastatic potential as previously reported (Nakano et al., 2003).

To clarify the factors that determine the metastatic potential of HuO9 sublines, we compared expression patterns of phosphotyrosine-containing proteins between low- and high-metastatic sublines (Figure 1). General enhancement of tyrosine phosphorylation was observed in high-metastatic sublines, M112 and M132, as well as parental HuO9, which also has rather high metastatic potential (Nakano et al., 2003). Among several phosphotyrosine-containing proteins showing elevated phosphorylation in high-metastatic sublines, the most striking difference was a broad band around 70 kDa (marked b in Figure 1). In addition, there were several other minor phosphotyrosine-containing proteins differentially expressed between low- and high-metastatic sublines, such as proteins around 60 kDa (marked c in Figure 1) and 120-130 kDa (marked a in Figure 1). These differences in tyrosine phosphorylation were consistent at different time points after plating (6 hr and 24 hr) with and without fibronectin coating (Supplemental Figure 1 and data not shown).

As candidate proteins of the difference around 120-130 kDa tyrosine phosphorylation, $p130^{Cas}$ and FAK were examined using phospho-specific antibodies (Figure 2). $p130^{Cas}$ is a docking protein involved in the integrin signaling. We generated phospho-specific antibodies against several putative phosphorylation sites of $p130^{Cas}$ and used them for the analysis. As a result, elevated phosphorylation of Tyr 762 was found in high-metastatic sublines (2.5 times as much as low-metastatic sublines), while phosphorylation of Tyr 460 of $p130^{Cas}$ did not show obvious

correlation with metastatic potential (Figure 2A). Tyr 460 represents tandem YDXP motifs in the substrate domain of $p130^{Cas}$, which binds Crk (Sakai et al., 1994) or Nck (Schlaepfer et al., 1997), and Tyr 762 consists of YDYV motif, which serves as a Src binding site when phosphorylated (Nakamoto et al., 1996). Expression of $p130^{Cas}$ did not vary significantly among each subline (Figure 2A).

FAK is a non-receptor tyrosine kinase, which is also involved in the integrin signaling, and its Tyr 397 is autophosphorylated when FAK is activated (Schaller et al., 1994). The expression of FAK and phosphorylation on Tyr 397 of FAK were analyzed. However, no remarkable elevation of tyrosine phosphorylated FAK was detected in high-metastatic sublines (Figure 2B).

To identify the phosphotyrosine-containing protein around 60 kDa, the expression level and tyrosine phosphorylation of Src family kinases was examined. Among the members of Src family kinases, only Fyn kinase had the tendency of hyperphosphorylation in high-metastatic sublines (Figure 2C). Tyrosine phosphorylation of c-Src, Yes, and Fgr, other members of Src family kinases that were examined, did not correlated with the metastatic potential (data not shown). However, absorption of Fyn by anti-Fyn antibody from lysates of low- and high-metastatic sublines could not removed the difference in tyrosine phosphorylation around 60 kDa (data not shown), indicating that not only Fyn contributes to the elevation of tyrosine phosphorylation around 60 kDa.

Overexpression and hyperphosphorylation of paxillin in high-metastatic HuO9 sublines.

From the molecular size and the broad appearance of the 70 kDa protein, we estimated that this highly phosphorylated protein in high-metastatic sublines was paxillin. Using a specific antibody of phospho-paxillin (Tyr 118) for the blotting of whole cell lysates, it was confirmed that high-metastatic sublines indeed contained a higher amount of tyrosine phosphorylated paxillin in high metastatic sublines (Figure 3A). It was also found that total paxillin expression was elevated in high-metastatic sublines (Figure 3A). As for both total paxillin and phospho-paxillin, high-metastatic sublines were estimated to contain about three to five times as much as low-metastatic sublines using densitometric analysis.

Absorption of paxillin by anti-paxillin antibody from lysates of low- and high-metastatic sublines removed most of the difference in tyrosine phosphorylation around 70 kDa (Figure 3B), indicating that paxillin mainly contributes to the elevation of tyrosine phosphorylation around 70 kDa.

Immunostaining of paxillin revealed that total paxillin and phospho-paxillin (Tyr 118) localize at focal adhesions, which were characterized at both ends of the actin filaments in L12 and M132 cells (Figure 3C). There was no significant change in the localization of paxillin by the metastatic potential of sublines, although the staining of total paxillin and phospho-paxillin were stronger in high-metastatic sublines than those in low-metastatic sublines (Figure 3D).

Src family kinase activity is elevated in the high-metastatic sublines

The general enhancement of tyrosine phosphorylation in high-metastatic sublines (Figure 1) suggests that the activity of some tyrosine kinases were enhanced in high-metastatic sublines. Therefore, we examined which tyrosine kinase is responsible for the high metastatic potential.

First, the difference in Src family kinase activity was investigated using Src-2 antibody, which is known to recognize wide ranges of Src family kinases. As a result, the activity of Src family kinases was elevated in the high-metastatic sublines (Figure 4A). The candidate for the Src family kinase responsible for the elevated kinase activity in high-metastatic sublines might be

Fyn, which showed enhanced autophosphorylation in high-metastatic sublines (Figure 2C). We also examined the kinase activity of FAK and c-Abl, which are also reported to phosphorylate the tyrosine residues of paxillin. However, we observed a lack of correlation between kinase activity of FAK or c-Abl and metastatic potential (Figure 4B).

To check the influence of Src family kinase activity on cell motility elevated in high-metastatic sublines, cell migration assay was performed. In the high-metastatic sublines treated with PP2, an inhibitor of Src family kinases, motility was significantly suppressed, while in the cells treated with PP3, inactive structural analog of PP2, their motility was not affected (Figure 4C). The effect of Src family kinase on the tyrosine phosphorylation of paxillin was also evaluated. When, high metastatic sublines were treated with PP2, the tyrosine phosphorylation of paxillin was almost completely abolished, while the phosphorylation remained unchanged when the cells were treated with PP3 (Figure 4D). These results indicate that, in high-metastatic sublines of HuO9, tyrosine phosphorylation of paxillin and enhanced cell motility are mostly dependent on the activity of Src family kinases.

Cell migration was attenuated by knocking down of paxillin expression in high-metastatic sublines

To evaluate the direct involvement of paxillin in the cell motility of the osteosarcoma cells, paxillin expression was knocked down using RNAi in high-metastatic HuO9 sublines. Using a novel approach called the Dicer method to introduce a series of siRNA into the cells, paxillin expression was suppressed by about 60%, while phospho-paxillin decreased by about 30% compared with LacZ siRNA treated cells (Figure 5A).

Although the expression of paxillin was not completely suppressed, cell motility was impaired by about two thirds by treatment with paxillin siRNA when compared with LacZ siRNA treated cells (Figure 5B). This difference is statistically significant over nonspecific effects of siRNA on cell survival and motility.

This attenuation of motility was not observed when the expression of $p130^{Cas}$ was knocked down using the Dicer method in high-metastatic sublines (Supplement Figure 2A, B). These results indicate paxillin rather than $p130^{Cas}$ is more closely associated with the motility of osteosarcoma sublines.

Overexpression of paxillin and elevation of Src family kinase activity synergistically enhance the motility of human osteosarcoma

To further examine the role of paxillin and its tyrosine phosphorylation on the motility of osteosarcoma sublines, the effect of transient transfection of GFP-paxillin and its phenylalanine mutant of two tyrosines (2F mutant) was evaluated. In 2F mutant, two critical tyrosine phosphorylation sites at Tyr 31 and Tyr 118 were mutated to phenylalanine, and these tyrosine residues were confirmed to be major phosphorylation sites by transient transfection of GFP-paxillin and GFP-2F mutant to COS-7 cells (Figure 6A).

Next, GFP-paxillin and GFP-2F mutant were transiently expressed in the low-metastatic subline, L12 (Figure 6B, arrowhead in lower panel). The tyrosine phosphorylation of GFP-paxillin was detected by phospho-paxillin (Tyr 118) antibody in L12 (Figure 6B, arrowhead in upper panel), though this polyclonal antibody showed slight reactivity even to the 2F mutant of paxillin. Both GFP-paxillin and GFP-2F mutant were confirmed to localize at focal adhesions (Figure 6C).

Cell motility was enhanced by the transient expression of GFP-paxillin compared with the

transfection of GFP-2F mutant or empty vector (Figure 6D). This indicates the amount of wild type paxillin is positively correlated with the motility of osteosarcoma sublines. Considering that GFP-2F mutant could localize at focal adhesions (Figure 6C), the lack of motility promoting effect of GFP-2F mutant was due to the absence of phosphorylation at Tyr 31 and Tyr 118.

The synergistic effect of paxillin overexpression and Src family kinase activity was examined using a low-metastatic subline, L12. We established L12 cells that stably express more than five times as much amount of exogenous paxillin as the wild type L12 subline, which is a similar level of endogenous paxillin in the high-metastatic sublines. FLAG epitope-tagged Fyn was transiently transfected to wild type L12 cells and paxillin overexpressing L12 cells (Figure 6E). Enhancement of tyrosine phosphorylation of paxillin was observed in Fyn-FLAG transfected cells compared with mock transfected cells in both wild type L12 and paxillin overexpressing L12 cells (Figure 6F). Cell migration assay reveals that overexpression of both Fyn-FLAG and paxillin-FLAG significantly enhances the cell motility of L12 cells (Figure 6G). This result of cell migration was correlated with the amount of phospho-paxillin in the cells (Figure 6F, upper panel), which suggests that overexpression of paxillin and Fyn contributes to the enhanced motility through the tyrosine phosphorylation of paxillin.

Discussion

We have shown the general enhancement of tyrosine phosphorylation in high-metastatic HuO9 sublines, and the elevated activation of Src family kinase. Among the substrates of Src family kinase, prominent phosphorylation of paxillin along with elevated expression of paxillin was observed in the high-metastatic sublines.

Since human osteosarcoma cell lines suitable for metastatic study were not available, results of previous biochemical analysis on metastatic osteosarcoma were derived from murine models (Iwaya et al., 2003; Khanna et al., 2001; Khanna et al., 2004). The present study is the first biochemical analysis on human metastatic osteosarcoma. We used four independent, but genetically close sublines of osteosarcoma which are excellent tools for analysis of signal alteration in the process of acquiring metastatic potential. The high-metastatic sublines were established by *in vivo* selection and the low-metastatic sublines by the dilution plating method. Considering that malignant tumors contain subpopulations of different metastatic capabilities, these selection methods resemble authentic events during the progression of osteosarcoma. Moreover, these sublines were established without any manipulation of genes, which minimizes the artificial effects on our study.

In these sublines of human osteosarcoma, the results of cell motility assay clearly reflected metastatic potential (Nakano et al., 2003). This is reasonable because the properties of cancer cells measured by cell migration assay such as cell movement and ability to interact with extracellular matrix are critical factors during tumor metastasis. Therefore in this study, cell motility was used as an indicator of metastatic potential.

Elevation of Src family kinase activity in metastases was reported in human colorectal cancer (Talamonti et al., 1993) and in human melanoma (Marchetti et al., 1998). According to these reports, there is clear difference in the activated member of Src family kinase among types of tumors. Talamonti et al. showed increased activity of c-Src in liver metastases compared to primary tumor. Marchetti et al. used brain metastatic sublines and found that kinase activity of

Yes, not c-Src, was elevated compared to low-metastatic cells. We recently reported that, in a metastatic model of murine melanoma cell lines, kinase activity of Fyn was elevated in high-metastatic sublines, and interacted with cortactin (Huang et al., 2003). Although not as significant as in the case of murine melanoma, Fyn will also be a candidate for the responsible kinase for metastatic potential of human osteosarcoma. Other members of Src family kinase with relatively low expression, such as c-Src, or with relatively low kinase activity do not appear to be involved in regulation of metastatic potential.

In osteosarcoma, elevated phosphorylation of YDYV motif in $p130^{Cas}$ in high-metastatic sublines (Figure 2A) is a possible clue to Src family activation because phosphorylated YDYV motif in $p130^{Cas}$ stabilizes the active form of Src family kinases by binding with the SH2 domain of Src family kinases (Burnham et al., 2000; Nakamoto et al., 1996). This type of molecule may function as a regulator of Src family kinases that causes activation of Src family kinases in osteosarcoma cells, though the cotribution of phosphorylated $p130^{Cas}$ may be low considering the small effect of RNAi on the cell motility.

Although this is the first report on hyperphosphorylation of paxillin in metastatic tumor, some studies investigated the relationship of cell motility and tyrosine phosphorylation of paxillin. Tyr 31 and Tyr 118 of paxillin are phosphorylated upon cell adhesion (Burridge et al., 1992) and Src family tyrosine kinases (Klinghoffer et al., 1999), FAK (Schaller & Parsons, 1995), and c-Abl (Lewis & Schwartz, 1998) are reported to phosphorylate these sites. The roles of phospho-paxillin on cell motility are still controversial. Migration promoting effect of phospho-paxillin was demonstrated by using Nara bladder tumor II (NBT II) cells (Petit et al., 2000), while migration inhibitory effect was shown by using NMuMG cells, MM-1 cells, and Cos 7 cells (Tsubouchi et al., 2002; Yano et al., 2000). Our results have added another example of the migration promoting effects of phospho-paxillin.

The migration promoting effect of phospho-paxillin might be due to interaction with Crk (Schaller & Parsons, 1995). Crk interacts with a cellular protein DOCK180, which binds directly and activates small GTPase Rac1 (Kiyokawa et al., 1998). Activation of this pathway provides a link between paxillin-Crk association and cell motility.

The binding partners of phospho-paxillin seem to be vary among tumor types and may provide some clue for the controversy between migration promoting and inhibitory effect of phospho-paxillin. In NMuMG cells, in which phosho-paxillin exerts migration inhibitory effect, phospho-paxillin was shown to bind p120RasGAP and RhoA activity was suppressed as a downstream of signal transduction (Tsubouchi et al., 2002). Therefore, it is also possible that SH2 domain-containing molecule other than Crk may function as binding partner of phospho-paxillin and send positive signal for cell motility in osteosarcoma cells.

We observed the impaired motility by knocking down the expression of paxillin and showed the direct effect of paxillin on cell migration. Paxillin knocked down cells showed 67% migration activity compared to LacZ siRNA treated cells. One reason for this rather weak motility suppression is the partial effect of RNAi, as 40% of paxillin and 68% of phospho-paxillin remained after the treatment with paxillin siRNA compared to LacZ siRNA treated cells. Another possible reason is the existence of other factors that enhance the metastatic potential independently of paxillin. However, considering the partial effect of RNAi, it can be estimated that paxillin has a significant contribution to high-metastatic phonotype.

We examined the contribution of $p130^{Cas}$, which is another substrate of Src family kinase and involved in the integrin signaling. As a result, suppression of $p130^{Cas}$ expression did not affect the motility of high-metastatic osteosarcoma cells, which supports the relative importance of

paxillin in the motility of osteosarcoma cells.

FAK is also known as a binding partner and a substrate of Src family kinase. However, in the osteosarcoma sublines, the tyrosine phosphorylation of FAK was not correlated with the activity of Src family kinase. This may suggest that, in the case of human osteosarcoma, the phosphorylation of FAK reflects other kinase activity including autophosphorylation and not strongly associated with metastatic potentials.

We have shown the migration promoting effect of phosho-paxillin by overexpression of GFP-paxillin and its mutant. Expression of exogenous GFP-paxillin enhanced the cell motility in the low-metastatic subline, while expression of GFP-2F muntants did not. Furthermore, we showed paxillin overexpression and Src family activity could contribute the high metastatic potential of osteosarcoma. Expression of Fyn-FLAG and paxillin-FLAG at the same time in the L12 subline promoted the motility synergistically, although it did not enhance the motility to the extent of high-metastatic sublines, probably because of the existence of other factors which contribute to the high-metastatic potential of osteosarcoma. These results strongly suggest that this cooperative function of Src family kinase and paxillin also works in endogenously expressed proteins and play a major role in high-metastatic phenotype of osteosarcoma cells.

Then, what is the mechanism of overexpression of paxillin in high-metastatic sublines of human osteosarcoma? The locus of paxillin, 17p8q, is not included in the areas where comparative genomic hybridization (CGH) analysis revealed gene amplification is frequent in human osteosarcoma (Batanian et al., 2002; Lau et al., 2004; Squire et al., 2003). Paxillin mRNA in high-metastatic sublines is at most 1.7 times compared to that in low-metastatic sublines by cDNA microarray analysis (Nakano et al., personal communication). Considering high-metastatic sublines express about five times as much paxillin as low-metastatic sublines, paxillin may be highly stable and degraded slowly in high-metastatic sublines.

In conclusion, this study provides information on the importance of phospho-paxillin during metastasis of human osteosarcoma. We have shown that enhancement of Src family kinase activity and overexpression of paxillin synergistically contribute to the high metastatic potential of human osteosarcoma through hyperphosphorylation of paxillin. Further biochemical analysis is needed to clarify the phosphotyrosine dependent binding partner with paxillin, since the downstream pathway specific to tumor metastasis is a potential therapeutic target. If Src family kinases are activated by a specific mechanism in metastatic osteosarcoma, that would also be an attractive therapeutic target. These themes deserve investigating to improve the extremely poor prognosis of metastatic osteosarcoma.

Materials and Methods

Antibodies and reagents

Anti-phosphotyrosine antibody 4G10 was purchased from Upstate Biotechnology. Phospho-specific antibodies against Tyr 460 and Tyr 762 of $p130^{Cas}$ were raised by immunizing rabbits with peptide CAEDVYDVP and CMEDYDYVHL respectively, and affinity purified. As anti-$p130^{Cas}$ antibody, polyclonal Cas2 antibody was used as described previously (Sakai et al., 1994). Monoclonal antibody against FAK was from BD Transduction Laboratories. Polyclonal antibody against phospho-FAK (Tyr 397) was purchased from Upstate Biotechnology. Monoclonal antibody against c-Src (GD11) was from Upstate Biotechnology. Polyclonal antibodies against Fyn (Fyn-3), Fgr (N-47) and pan-Src (Src-2) were from Santa Cruz

Biotechnology. Monoclonal antibodies against Yes, Hck, Lck and Lyn were purchased from BD Transduction Laboratories. Monoclonal antibody against paxillin was from Zymed Laboratories Inc. Polyclonal antibody against phospho-paxillin (Tyr 118) was purchased from Cell Signaling. Anti-a-tubulin antibody (B-5-1-2) was purchased from SIGMA. Monoclonal antibody against Abl was from BD Biosciences. Polyclonal antibody against GFP (598B) was from Medical and Biological Laboratories. HRP-conjugated anti-mouse antibody was purchased from Amersham Pharmacia. Alexa Fluor 488 goat anti-mouse IgG, Alexa Fluor 594 goat anti-rabbit IgG and Alexa Fluor 546 phalloidin were purchased from Molecular Probe. Normal rabbit serum was from DakoCytomation. Src family kinase inhibitor 4-amino-5-(4-cholorophenyl)-7-(t-butyl)pyrazolo[3,4-d]pyrimidine (PP2) and the structural analog 4-amino-7-phenylpyrazol [3,4-d]pyrimidine (PP3) were purchased from Calbiochem-Novabiochem Ltd.

Plasmids

A FLAG epitope-tagged paxillin construct was generated by amplifying the coding sequence of human paxillin by PCR using the primers 5'-CGTACCTCGAGGCCATGGACGACCTCGACGC-3' and 5'-GGAATTCATTTGTCGTCGTCGTCCTTGTAGTCGCAGAAGAGCTTGAGGAAGC-3'. This resulted in a fragment with an Xho I site (underlined), a sequence encoding the FLAG epitope (DYKDDDDK), followed by a termination codon and an EcoRI site (underlined). This fragment was then digested with XhoI and EcoRI sequentially, and ligated into the mammalian expression vector pcDNA3.1(-)/Myc-His B (Invitrogen).

GFP-paxillin is a kind gift from Dr. Y. Sawada (Department of Biological Sciences, Columbia University). Phenylalanine mutant at Tyr 31 and Tyr 118 was generated by amplifying GFP-paxillin with following primers. 5'-CGGCCTGTGTTCTTAAGCGAGGAGACCCCCTTCTCATACCCAAC-3' and 5'-GTTGGGTATGAGAAGGGGGTCTCCTCGCTTAAGAACACAGGCCG-3' were used for Tyr 31, and 5'-CCGTGCTCTAGAGTGGGAGAGGAGGAGCACGTGTTCAGCTTCCC-3' and 5'-GGGAAGCTGAACACTGTCTCCTCCTCTCCCACTCTAGAGCACGG-3' were used for Tyr 118.

A FLAG epitope tagged Fyn construct was generated by amplifying the RT-PCR product of human colon cancer cell line, HCT116, by PCR using the primers 5'-GGATCCATGGGCTGTGTGCAATGTAAG-3' and 5'-GTTAACTCACTTGTCGTCATCGTCCTTGTAGTCCAGGTTTTCACCAGGTTG-3'. This PCR product was firstly inserted into pGEM-T Easy vector (Promega), followed by excision with EcoRI, and ligated into the mammalian expression vector pcDNA3.1(-)/Myc-His A (Invitrogen).

Cell culture and transfection

A human osteosarcoma cell line, HuO9, and its high-metastatic (M112, M132) and low-metastatic sublines (L12, L13) have been described previously (Nakano et al., 2003). Osteosarcoma cells were maintained in RPMI 1640 medium with 10% FBS at 37 _ with 5% CO_2. Cos-7 cells were maintained in Dulbecco's Modified Eagle's medium (DMEM) with 10% FBS at 37_ with 5% CO_2. Transfection was performed by using FuGENE 6 (Roche) according to the manufacturer's instruction. Selection of clones was performed by using geneticin (Sigma) at the concentration of 30 μg/ml.

Immunoblotting and Immunoprecipitation

Before extracting cell lysates, osteosarcoma cells were cultured for at least 48 hr to ensure complete cell adhesion to culture dishes unless otherwise indicated. Cells were lysed in 1% Triton X-100 buffer (50 mM Hepes, 150 mM NaCl, 10% glycerol, 1% Triton-X 100, 1.5 mM $MgCl_2$, 1 mM EGTA, 100 mM NaF, 1 mM Na_3VO_4, 10 μg/ml aprotinin, 10 μg/ml leupeptin, 1 mM phenylmethylsulfonyl fluoride), and insoluble materials were removed by centrifugation. To investigate the effect of PP2 treatment, cells were treated with 10 μM of PP2 or 10 μM of PP3 for 30 min prior to harvesting cells.

Protein concentration was measured by BCA Protein Assay (PIERCE) and the protein aliquots were separated by SDS-PAGE. Gels were transferred to a polyvinylidene difluoride membrane (Millipore) and subjected to immunoblotting. After blocking in 5% skim milk / TBST (100 mM Tris-HCl pH 8.0, 150 mM NaCl, 0.05% Tween 20) for 1 hr, blots were incubated with appropriate primary antibodies. In case of 4G10 stain, blocking was performed with 5% BSA was used instead of skim milk. Blots were then washed three times with TBST, incubated with HRP-conjugated secondary antibodies for 30 min, washed twice by TBST and twice with TBS (100 mM Tris-HCl pH 8.0, 150 mM NaCl), and visualized by autoradiography using chemiluminescence reagent (Western Lighting, Perkin Elmer).

The images were captured by molecular imager GS800 (BIO-RAD) and the density of each smear was quantified by Quantity One (BIO-RAD).

For immunoprecipitation, aliquots of protein were mixed with appropriate antibodies and incubated for 1 hr on ice. Then samples were rotated with protein A- or protein G-sepharose beads (Amersham Pharmacia) for 2 to 12 hr at 4 _. After the beads were washed four times with 1% Triton-X 100 buffer, the samples were boiled in sample buffer (0.1 M Tris HCl pH 6.8, 2% SDS, 0.1 M dithiothreitol, 10% glycerol, 0.01% bromophenol blue) for 5 min and analyzed by SDS-PAGE.

Immunocytochemistry

Cells were grown on 12-mm circle cover glasses (Fisher) in 24 well plates, washed three times with PBS, fixed with 4% paraformaldehyde / 0.1 M phosphate buffer for 5 min at room temperature, washed once with PBS, and permeabilized with 0.2% Triton-X 100 in PBS for 10 min. After another washing step with PBS and blocking in 5% goat serum and 3% BSA / TBST for 30 min, cells were incubated with anti-paxillin antibody (1:2000) and anti phospho-paxillin antibody (1:250) in 5% goat serum and 3% BSA / TBST for 1 hr at room temperature. Cells were washed three times with PBS and incubated with appropriate second antibodies (Molecular Probe) (1:2000) in 5% goat serum and 3% BSA / TBST. When actin was stained with phalloidin, Alexa Fluor phalloidin was combined with second antibody at the concentration of 1 U/ml.

After cells were washed three times with PBS, cover glasses were mounted in 1.25% DABCO, 50% PBS, 50% glycerol and visualized using a Radiance 2100 confocal microscopic system (BIO-RAD).

In vitro kinase assay

For kinase assay, fresh cell lysate was prepared and mixed with the antibody of interest for 1 hr on ice. Then samples were rotated with protein A-sepharose or protein G-sepharose for 1 hr at 4 _. The beads were consequently washed with 1% Triton-X 100 buffer and kinase buffer (50 mM Tris HCl, pH 7.4, 50 mM NaCl, 10 mM $MgCl_2$, 10 mM $MnCl_2$) three times respectively.

Kinase reaction was performed in 30 μl of kinase buffer with 10 μg of synthetic polypeptides poly[Glu-Tyr](4:1) (Sigma) as exogenous substrate and 5 μCi of [γ-32P]ATP (ICN) at room temperature for 1 hr. Kinase reaction was stopped by the addition of SDS-PAGE sample buffer (0.1 M Tris HCl pH 6.8, 2% SDS, 0.1 M dithiothreitol, 10% glycerol, 0.01% bromophenol blue). The samples were boiled for 5 min and analyzed by SDS-PAGE using 8% polyacrylamide gel. The gels were then dried and exposed to autoradiography. The images were captured by molecular imager GS800 (BIO-RAD) and the density of each smear (area shown by a bracket) was quantified by Quantity One (BIO-RAD).

Cell migration assay

Cell migration assay was performed by using Cell Culture Insert with 8.0 μm pore size PET filter (Becton Dickinson). Prior to the assay, the lower surface of the filter was immersed for 30 min in 10 μg/ml fibronectin (Sigma) diluted with PBS. Next, 700 μl of RPMI 1640 medium with 10% FCS was added to the lower chamber. Then, 5_10^4 cells were suspended in 300 ml of RPMI 1640 medium with 10% FCS and added to the upper chamber.

After incubation for 24 hr at 37 _ in a humid 5% CO_2 atmosphere, the cells on the upper surface of the filter were completely removed by wiping with cotton swabs. The cells on the lower surface of the filter were fixed in methanol for 30 min, washed with PBS, and then stained with Giemsa's stain solution (Muto Pure Chemicals Co. Ltd.) for 30 sec. After washing three times with PBS, the filters were mounted on a glass slide. The cells on the lower surface were counted from photographs taken of at least five fields at a magnification of 200_ under the microscope. Student's *t*-test was used to analyze data from these experiments. To investigate the effect of PP2 treatment, cells were allowed to migrate in the presence of 10 μM of PP2 or 10 μM of PP3.

RNAi analysis

Short interfering RNA (siRNA) of human paxillin and $p130^{Cas}$ was generated using BLOCK-iT RNAi TOPO Transcription Kit and BLOCK-iT Complete Dicer RNAi Kit (Invitrogen) according to the manufacturer's instructions. In the generation of siRNA for paxillin, 936 bp from the intiation codon of human paxillin were chosen as the target sequence, and amplified by PCR using the primers, 5'-ATGGACGACCTCGACGCC-3' and 5'-GTTCAGGTCAGACTGCAGGC-3'. As for $p130^{Cas}$, 866 bp was chosen as the target sequence, and amplified with the primers, 5'-ACACCATGAACCACCTGAACGTG-3' and 5'-ATACACCTCCAGCAACGGGT-3'.

Short interfering RNA (siRNA) of LacZ was generated in the same procedure as paxillin siRNA, and was used as a negative control. Transfection was performed with Lipofectamine 2000 (Invitrogen) and the effect was analyzed at 72 hr after the transfection.

Acknowledgements

We are grateful to Dr. Y. Sawada (Department of Biological Sciences, Columbia University) for donating paxillin cDNA.

K.A. is an awardee of the Research Resident Fellowship from the Foundation for Promoting of Cancer Research (Japan) for the 3rd Term Comprehensive 10-Year-Strategy for Cancer Control.

This study was supported by the Program for Promotion of Fundamental Studies in Health Science of Pharmaceuticals and Medical Devices Agency (PMDA).

References

Batanian, J.R., Cavalli, L.R., Aldosari, N.M., Ma, E., Sotelo-Avila, C., Ramos, M.B., Rone, J.D., Thorpe, C.M. & Haddad, B.R. (2002). *Mol Pathol*, **55,** 389-93.

Burnham, M.R., Bruce-Staskal, P.J., Harte, M.T., Weidow, C.L., Ma, A., Weed, S.A. & Bouton, A.H. (2000). *Mol Cell Biol*, **20,** 5865-78.

Burridge, K., Turner, C.E. & Romer, L.H. (1992). *J Cell Biol*, **119,** 893-903.

Huang, J., Asawa, T., Takato, T. & Sakai, R. (2003). *J Biol Chem*, **278,** 48367-76.

Huth, J.F. & Eilber, F.R. (1989). *Arch Surg*, **124,** 122-6.

Iwaya, K., Ogawa, H., Kuroda, M., Izumi, M., Ishida, T. & Mukai, K. (2003). *Clin Exp Metastasis*, **20,** 525-9.

Khanna, C., Khan, J., Nguyen, P., Prehn, J., Caylor, J., Yeung, C., Trepel, J., Meltzer, P. & Helman, L. (2001). *Cancer Res*, **61,** 3750-9.

Khanna, C., Wan, X., Bose, S., Cassaday, R., Olomu, O., Mendoza, A., Yeung, C., Gorlick, R., Hewitt, S.M. & Helman, L.J. (2004). *Nat Med*, **10,** 182-6.

Kimura, K., Nakano, T., Park, Y.B., Tani, M., Tsuda, H., Beppu, Y., Moriya, H. & Yokota, J. (2002). *Clin Exp Metastasis*, **19,** 477-85.

Kiyokawa, E., Hashimoto, Y., Kobayashi, S., Sugimura, H., Kurata, T. & Matsuda, M. (1998). *Genes Dev*, **12,** 3331-6.

Klinghoffer, R.A., Sachsenmaier, C., Cooper, J.A. & Soriano, P. (1999). *Embo J*, **18,** 2459-71.

Lau, C.C., Harris, C.P., Lu, X.Y., Perlaky, L., Gogineni, S., Chintagumpala, M., Hicks, J., Johnson, M.E., Davino, N.A., Huvos, A.G., Meyers, P.A., Healy, J.H., Gorlick, R. & Rao, P.H. (2004). *Genes Chromosomes Cancer*, **39,** 11-21.

Lewis, J.M. & Schwartz, M.A. (1998). *J Biol Chem*, **273,** 14225-30.

Marchetti, D., Parikh, N., Sudol, M. & Gallick, G.E. (1998). *Oncogene*, **16,** 3253-60.

Meyers, P.A., Heller, G., Healey, J.H., Huvos, A., Applewhite, A., Sun, M. & LaQuaglia, M. (1993). *J Clin Oncol*, **11,** 449-53.

Nakamoto, T., Sakai, R., Ozawa, K., Yazaki, Y. & Hirai, H. (1996). *J Biol Chem*, **271,** 8959-65.

Nakano, T., Tani, M., Ishibashi, Y., Kimura, K., Park, Y.B., Imaizumi, N., Tsuda, H., Aoyagi, K., Sasaki, H., Ohwada, S. & Yokota, J. (2003). *Clin Exp Metastasis*, **20,** 665-74.

Pawson, T. (2004). *Cell*, **116,** 191-203.

Petit, V., Boyer, B., Lentz, D., Turner, C.E., Thiery, J.P. & Valles, A.M. (2000). *J Cell Biol*, **148,** 957-70.

Sakai, R., Iwamatsu, A., Hirano, N., Ogawa, S., Tanaka, T., Mano, H., Yazaki, Y. & Hirai, H. (1994). *Embo J*, **13,** 3748-56.

Schaller, M.D. (2001). *Oncogene*, **20,** 6459-72.

Schaller, M.D., Hildebrand, J.D., Shannon, J.D., Fox, J.W., Vines, R.R. & Parsons, J.T. (1994). *Mol Cell Biol*, **14,** 1680-8.

Schaller, M.D. & Parsons, J.T. (1995). *Mol Cell Biol*, **15,** 2635-45.

Schlaepfer, D.D., Broome, M.A. & Hunter, T. (1997). *Mol Cell Biol*, **17,** 1702-13.

Squire, J.A., Pei, J., Marrano, P., Beheshti, B., Bayani, J., Lim, G., Moldovan, L. & Zielenska, M. (2003). *Genes Chromosomes Cancer*, **38,** 215-25.

Talamonti, M.S., Roh, M.S., Curley, S.A. & Gallick, G.E. (1993). *J Clin Invest*, **91,** 53-60.

Tsubouchi, A., Sakakura, J., Yagi, R., Mazaki, Y., Schaefer, E., Yano, H. & Sabe, H. (2002). *J Cell Biol*, **159,** 673-83.

Tsuchiya, H., Kanazawa, Y., Abdel-Wanis, M.E., Asada, N., Abe, S., Isu, K., Sugita, T. & Tomita, K. (2002). *J Clin Oncol*, **20,** 3470-7.
Turner, C.E. (2000). *Nat Cell Biol*, **2,** E231-6.
Ward, W.G., Mikaelian, K., Dorey, F., Mirra, J.M., Sassoon, A., Holmes, E.C., Eilber, F.R. & Eckardt, J.J. (1994). *J Clin Oncol*, **12,** 1849-58.
Yano, H., Uchida, H., Iwasaki, T., Mukai, M., Akedo, H., Nakamura, K., Hashimoto, S. & Sabe, H. (2000). *Proc Natl Acad Sci U S A*, **97,** 9076-81.
Yeatman, T.J. (2004). *Nat Rev Cancer*, **4,** 470-80.

Legends to Figures

Figure 1

Elevated tyrosine phosphorylation of several proteins in high-metastatic sublines of HuO9 cells.

Low-metastatic sublines (L12, L13), high-metastatic sublines (M112, M132) and parental HuO9 cells plated on plastic culture dishes for longer than 48 hr were lysed for immunoblotting with anti-phosphotyrosine antibody 4G10. Hyperphosphorylated proteins in high-metastatic sublines are indicated on the right (a, b, c).

Figure 2

Elevated tyrosine phosphorylation of p130^{Cas} (Tyr 762) in high-metastatic sublines.

A: Whole cell lysates from low-metastatic (L12, L13) and high-metastatic sublines (M112, M132) were immunoblotted for two kinds of anti-phosho-p130^{Cas} antibody (Tyr 460 representing the tandem YDXP motif, and Tyr 762 representing the YDYV motif in Src binding domain) and p130^{Cas} antibody. Density of each blot was measured as described in Materials and Methods.

B: Whole cell lysates from low-metastatic (L12, L13), high-metastatic (M112, M132) and parental HuO9 were immunoblotted for anti-phospho-FAK antibody (Tyr 397) and anti-FAK antibody. Density of each blot was measured as described in Materials and Methods.

C: Fyn kinase of low- and high-metastatic sublines was immunoprecipitated by anti-Fyn polyclonal antibody and subsequently immunoblotted with anti-phosphotyrosine antibody 4G10 or anti-Fyn antibody.

Figure 3

Overexpression and hyperphosphorylation of paxillin in high-metastatic sublines.

A: Whole cell lysates from low-metastatic (L12, L13), high-metastatic (M112, M132) and parental HuO9 were immunoblotted for anti-phospho-paxillin antibody (Tyr 118), paxillin antibody, and anti-α-tubulin antibody as an internal control. Densities of paxillin and phospho-paxillin blots are shown on the right.

B: Whole cell lysates of low- and high-metastatic sublines and parental HuO9 cells were immunoprecipitated by monoclonal anti-paxillin antibody. Both immunoprecipitates and supernatants (indicated at the top) were subjected to immunoblotting analysis by anti-phosphotyrosine antibody 4G10 and anti-paxillin antibody.

C: L12 and M132 sublines were immunostained with anti-paxillin antibody (a, d: green), and chemically stained with phalloidin (b, e: red) at the same time.

D: Low- and high-metastatic sublines were immunostained with the antibody against paxillin (b-e: green) or phospho-paxillin (g-j: red). Superimposed confocal images (l-o: merge)